ORIGINAL ARTICLE

Surface-enhanced Raman spectroscopy (SERS) investigations of saliva for oral cancer diagnosis

A. Fălămaș [1] · H. Rotaru [2] · M. Hedeșiu [3]

Abstract

Saliva could be an optimal sample for non-invasive cancer detection, as it contains plenty of proteins and metabolites which can reflect the health status of an individual. Moreover, pairing it with high-sensitivity, label-free detection techniques could prove successful for early cancer diagnosis. In this study, we explore the enhancement of salivary characteristic Raman bands by using label-free, ultrasensitive surface-enhanced Raman scattering (SERS) based on gold nanoparticles. SERS maps were acquired from dry samples of saliva supernatant mixed with Au colloidal nanoparticles, which was then pipetted on clean glass slides. The SERS spectra presented a high variability of signal intensities and frequency shifts. However, several reproducible SERS spectra showing well-resolved bands were obtained at certain locations on the maps, where Au nanoparticles clustered together during the air-drying. The healthy and oral cancer saliva could be differentiated using principal components analysis based on several SERS bands assigned mainly to amino acids and proteins. Moreover, thiocyanate Raman modes were detected in saliva samples of both smoking and non-smoking volunteers and cancer patients. The analysis indicated that the cancer group displayed an overall higher level of the 2126 cm^{-1} band area assigned to C–N stretching vibrations of thiocyanate.

Keywords Surface-enhanced Raman spectroscopy · Saliva · Diagnosis · Oral cancer

Introduction

Oral cancer involving the lip and oral cavity is the sixth most common type of cancer worldwide [1]. Current diagnosis relies on clinical investigation and histopathological examinations, with a high risk of undetected cancerous lesions in hidden areas. Moreover, early detection is crucial for improving survival of patients. Therefore, there is a high need for non-invasive, high-specificity, and high-sensitivity detection methods [2].

The demands for ultra-sensitive detection methods may be met by Raman spectroscopy techniques. Normal Raman spectroscopy has several unique advantages, such as minimal or no sample preparation, high spatial resolution, no labels required, and molecular-level information [3]. Raman spectroscopy is based on the inelastic scattering of photons following the interaction with the vibrating atoms in the molecules [4]. The individual Raman bands observed in the spectrum are characteristic to specific molecular motions, offering thus an extraordinary chemical specificity of the sample. The use of Raman spectroscopy for the development of diagnostic methods is based on the fact that the molecular changes induced by diseases are reflected in the Raman spectra, leading to the possibility of highly specific fingerprinting of the biochemical composition of cells and tissues, which can then be used for cancer diagnosis applications [5, 6]. However, the Raman scattering from biological samples is usually weak and often overlapped with the background signal resulted from the intracellular biocomponents. To overcome these inconveniences, surface-enhanced Raman scattering (SERS) has been developed to enhance the Raman signal by

✉ A. Fălămaș
afalamas@itim-cj.ro

1 National Institute for Research and Development of Isotopic and Molecular Technologies, 67-103 Donat, 400293 Cluj-Napoca, Romania

2 Department of Oral and Maxillofacial Surgery, "Iuliu-Hateganu" University of Medicine and Pharmacy, Cluj-Napoca, Romania

3 Department of Oral Radiology, Faculty of Dental Medicine, "Iuliu-Hateganu" University of Medicine and Pharmacy, Cluj-Napoca, Romania

exploiting the interaction between the investigated molecules and the surface of metal nanoparticles [7, 8]. SERS has been lately used for a multitude of medical applications ranging from probing and imaging live cells [9], to ex vivo diagnosis [10, 11] and in vivo tumor targeting in live animals [12, 13].

Saliva provides several advantages which could make it an optimal sample for non-invasive cancer detection [14]. Proteins, nucleic acids, and enzymes found in saliva could be potential biomarkers for cancer detection, as they have been shown to have distinct levels in cancerous compared with healthy individuals [15]. Various cancers have been identified and diagnosed using saliva and methods such as liquid chromatography [16], mass spectrometry, and enzyme-linked immunosorbent assay (ELISA) [17]. Saliva can be easily and continuously collected during the treatment; it contains plenty of proteins and metabolites [18], which change accordingly with the disease transformations [19], and these modifications can be correlated with the SERS spectral features of saliva. SERS saliva has been investigated for the non-invasive detection and diagnosis of nasopharyngeal carcinoma [20], oral squamous cell carcinoma [21], lung cancer [22], Sjörgren's syndrome diagnosis [23], and benign and malignant breast tumor differentiation based on saliva proteins [24, 25]. Breast cancer was diagnosed based on the quantitative analysis of sialic acid concentration found in saliva; among 100 breast cancer patients, the concentration of sialic acid was around 6 times higher than that in healthy controls [26]. Lung cancer investigations based on saliva revealed the decrease of SERS peaks assigned to proteins and nucleic acids in lung cancer group compared with control [22]. Oral squamous cell carcinoma was diagnosed with 89% sensitivity and 73% accuracy using SERS on saliva samples and linear discriminant analysis [21].

The aim of the present study was to investigate the saliva signal using metal nanoparticles and SERS spectroscopy. We applied a simple method involving saliva supernatant mixed with gold (Au) nanoparticles and acquired SERS spectra from a drop of the mixture dried on glass slides. Additionally, we aimed to differentiate between the SERS signal of saliva collected from healthy volunteers and oral cancer–confirmed patients. Multivariate statistical techniques were employed to analyze and discriminate the SERS spectra from both groups.

Materials and methods

Saliva samples

Saliva samples were collected from five healthy individuals (2 females and 3 males) and six patients (2 females and 4 males) with a pathologically confirmed squamous cell carcinoma (SCC) of oral cavity. There were a similar number of smokers (2 healthy subjects and 3 patients with oral cancer) and non-

smokers (3 healthy volunteers and 3 patients) included in the study. The mean age of the volunteers was 40, while that of the cancer patients was 60 years old. The samples were collected before breakfast using Salimetrics passive drool collection kit, following rinsing of the mouth with water. The saliva was kept at − 80 °C until the day of analysis. After thawing at room temperature, it was centrifuged for 20 min at 9000 g and 10 °C to remove epithelial cells and other debris and obtain pure saliva. The supernatant was mixed in a 1:1 volume ratio with colloidal Au nanoparticles of 50-nm diameter acquired from Sigma. The Au nanoparticles were selected following several tests based on the highest enhancement of the Raman signal acquired from saliva samples. The nanoparticles were characterized by UV-Vis absorption spectroscopy (Jasco V550 Spectrophotometer) using 1-mm-long quartz cells (Supplementary Material, Fig. S1). The absorption maximum of the colloidal nanoparticles is observed at 540 nm.

The saliva–nanoparticles mixture was dropped on clean glass slides and allowed to dry at room temperature. Optical microscopy images revealed that the samples presented a ring at the edge of the dried drops, next to an unevenly coated region.

Surface-enhanced Raman spectroscopy measurements

The SERS experiments were carried out using a Renishaw inVia Raman microscope (Renishaw, PLC, New Mills Wotton-under-Edge, Gloucestershire, UK) equipped with a 785-nm diode laser with a maximum power of 300 mW and a grating of 1200 lines/mm. A neutral density filter was used to avoid sample photodegradation and only 10% of the laser power reached the sample. The instrument was wavelength calibrated using a silicon wafer. The spectra were acquired in the 600–1720 cm^{-1} wavenumber range using a 50X objective, 3s integration time, and 3 accumulations. SERS maps were collected from the edges of the mixture drops. A small area of a few tens of micrometers was selected from each sample for the acquisition of SERS maps. The maps consisted of approximately 30 to 80 spectra collected with a step size of 2 μm from healthy subjects and patients with oral cancer.

Additionally, extended SERS spectra were collected from 5 healthy saliva samples and 3 oral cancer ones in the 100–3200 cm^{-1} spectral range by using the same measurement system, in order to identify the thiocyanate band above 2000 cm^{-1}. The extended spectra were collected as time series of 5 spectra from the same location. At least two separate positions were selected from the dried spots on each sample. Each extended spectrum was obtained following 10s integration time and one accumulation. The mean profiles and standard deviations were calculated from 49 healthy SERS spectra and 30 oral cancer ones.

Data pre-processing and analysis

The pre-processing of the data sets was performed in Matlab and consisted of cosmic ray removal, background subtraction, and baseline correction. The lowest intensity spectrum found in the Raman map was subtracted from the entire data set to remove the background. The baseline correction was applied by fitting and subtracting a fifth-order polynomial from the data set. Mean intensity profiles were obtained for each group and the difference spectrum was calculated by subtracting the mean spectrum of the healthy group from the mean spectrum of the cancer group. Peak assignment was carried out based on the current literature in the field [22, 27, 28].

Principal components analysis (PCA) was employed for the data analysis. SERS maps were reproduced by plotting the scores of various principal components (PCs) at each position in the map where a SERS spectrum was acquired. The area of the 2126 cm^{-1} band was calculated for each acquired spectrum by delimiting the position of the peak and applying a baseline correction for that region.

Results and discussion

SERS analysis of saliva

An 18×12 μm area was selected from a sample collected from an oral cancer patient and SERS spectra in the 600–1720 cm^{-1} wavenumber range were collected with a 2-μm step size. A total of 54 spectra were acquired. The spectra presented an on and off blinking behavior, showing some SERS bands at one acquisition position and disappearing at the next, making it difficult to characterize the sample. The SERS variability was thus evidently displayed, as the intensity and band position of the spectra varied from one point of acquisition to another. Principal components analysis was applied to reduce the dimensionality of the data set. The first three PCs accounted for 97% of the variance in the data set and are displayed in Fig. 1a. Some common bands were observed: 620, 657, 740, 851, 947, 1044, 1075–1080, 1152, 1196, 1282, 1403, 1453–1462, and 1614 cm^{-1}. Based on the literature in the field, most of these peaks are assigned to proteins and amino acids; however, phospholipids and nucleic acids are also observed [20, 22, 27, 28].

We reproduced a SERS map (Fig. 1b) by plotting the scores of PC1 at each position in the map where a SERS spectrum was acquired. Figure 1c presents several SERS spectra collected from various locations on the map as indicated by the (x, y) positions in the figure's legend. As it can be observed from the color distribution associated to the SERS spectral intensity plotted in Fig. 1c, the highest intensity spectra were grouped around an area of the map. The SERS spectra collected from these points (e.g., positions (3,1) and (3,2))

showed high-intensity reproducible SERS spectra with well-resolved bands. Moving away from this area to a spot where the intensity in the SERS map is lower, a decreased intensity SERS spectrum was acquired, and the observed peaks shifted in frequency compared with the previous ones. Moving even further away from the initial location at position (7,4), a low signal-to-noise ratio spectrum was acquired, showing unresolved SERS bands. Considering this distribution of the SERS signal, we can presume that the Au nanoparticles clustered during the air-drying of the drop, which lead to fluctuations in signal intensities and frequencies. Therefore, the enhancement of the biomolecules present in the saliva supernatant is observed mainly at the locations where the Au nanoparticles accumulate forming "hot spots," which lead to strong enhancements of the Raman scattering. SERS spectra presented variability even at these locations, which could indicate that the enhancement of the Raman modes depends on the number of nanoparticles and the biomolecules present at the focal point of the laser, the interaction mode of the biomolecules with the nanoparticles (e.g., chemisorption, physisorption), and the various orientations of the species in respect to the nanoparticle surface [29].

A SERS map of 10×14 μm was acquired from a saliva sample collected from a healthy donor, as well (Fig. 2b). A similar blinking behavior of the SERS spectra was observed when analyzing each of them individually, as in the case of the previously analyzed SERS map. Following PCA, we reproduced a SERS map by plotting the first PC, which accounted for 90% of the total variance. High-intensity, well-resolved SERS peaks were observed in the spectra acquired from several positions that grouped together across the map, similarly to the previous case. The SERS spectra displayed in Fig. 2c clearly show that moving away from the place where the Au nanoparticles accumulated, the SERS intensity decreased. Different vibrational modes were enhanced in these SERS spectra, such as the 757 cm^{-1} assigned to tryptophan, 940 cm^{-1} assigned to amino acids and polysaccharides, 1067 cm^{-1} attributed to glucose and triglycerides, 1276 cm^{-1} where the amide III is observed or unsaturated fatty acids, and several bands in the 1430–1490 cm^{-1} spectral range where CH_2 bending mode of lipids and proteins, as well as amide II vibrational modes are present.

Thiocyanate detection

Based on the molecular vibrational assignment of the acquired SERS signal, we identified the 736 cm^{-1} band which may indicate the presence of thiocyanate in saliva. Thiocyanate (SCN^-) enters the human body through the intake of Brassica vegetables, milk, and cheese, and can be found in human serum, saliva, and urine. On the other hand, the level of thiocyanate ion can be used as an indicator of tobacco smoke exposure, as a product of cyanide and has been long
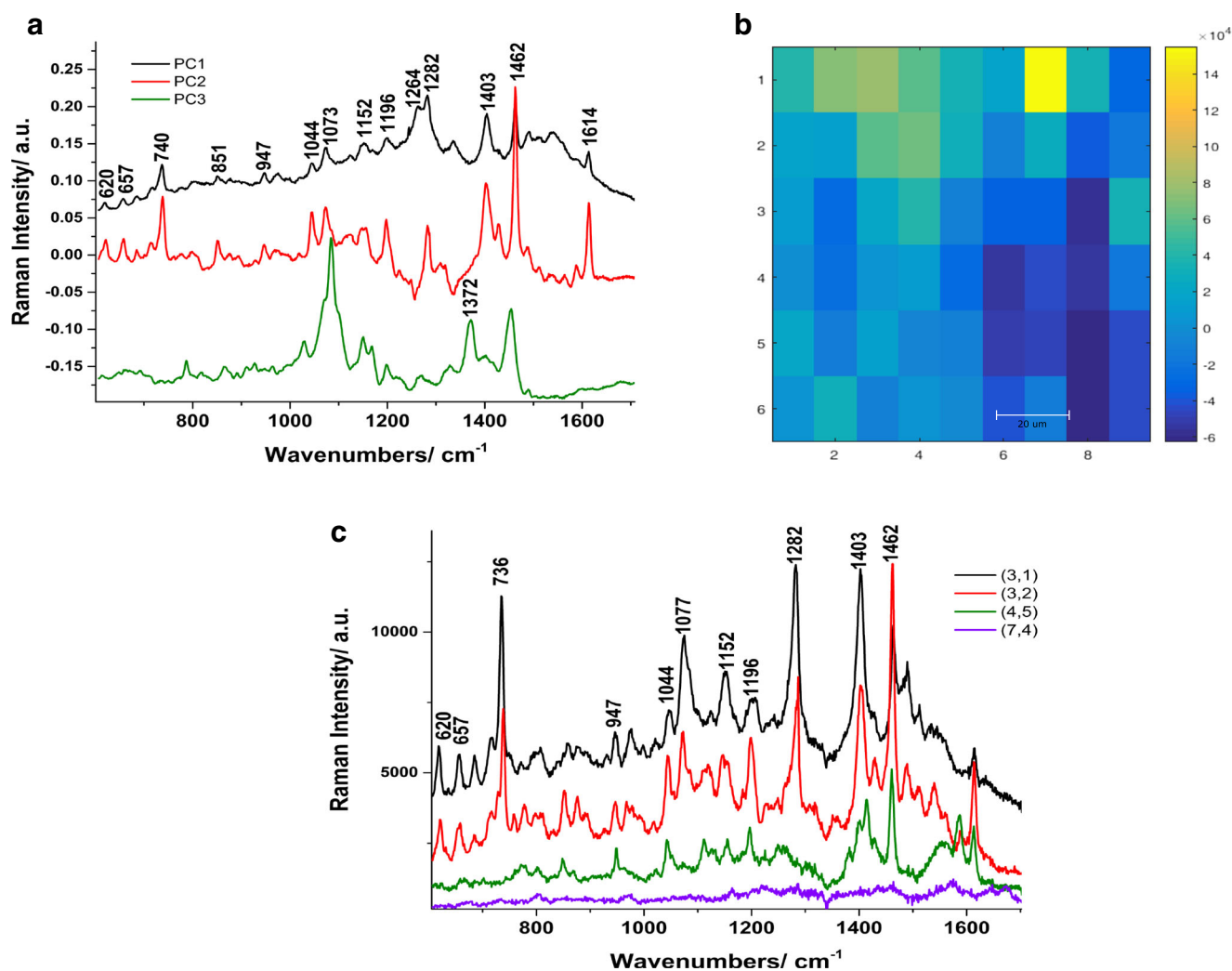
Fig. 1 a The loadings of the first three principal components characteristic to an oral cancer patient (PC1 91.5%, PC 4%, PC3 1.5%). PC1 and PC3 were vertically shifted for better visualization. b SERS map reproduced by plotting the score of PC1. The highest intensity is colored in yellow and the lowest intensity in dark blue. c SERS spectra collected from the positions with (x,y) coordinates indicated on the map

used for the discrimination between smokers and non-smokers [30]. This ion has been detected using SERS in milk [31], human serum and saliva samples [32], and human urine [35], and its adsorption modes on silver nanoparticles have been characterized [33]. Thiocyanate has three Raman active vibrations around 450, 747, and 2120 cm^{-1}. In order to examine if thiocyanate can truly be detected in our saliva samples, we acquired time series extended SERS spectra in the 100–3200 cm^{-1} wavenumber range, hoping to observe other vibrational modes of thiocyanate, as well. A total of 49 SERS spectra were collected from healthy saliva samples and 30 spectra from oral cancer samples. An example of the extended SERS spectra acquired at 10s intervals from each other is shown in Fig. 3a. Several bands were observed in all spectra, such as the 289, 450, 835, 1001, 1216, 1512, 1587, and 2126 cm^{-1}. These bands are assigned mainly to amino acids and proteins [27, 28], while the 2126 cm^{-1} band might be indicative of thiocyanate, based on the current literature in

the field [33]. This peak is assigned to C–N stretching vibrations of thiocyanate [34] and was identified in all of the extended SERS spectra acquired from both saliva groups. Thiocyanate can play the role of an important biomarker in human health and there is a real need for its rapid and reproducible analysis. Higher concentrations of thiocyanate in urine were associated with emphysema, cancer, and chronic bronchitis, indicating thus a significant risk effect of this ion's concentration on cancer and lung problems [35]. The intensity of the SERS peak around 2100 cm^{-1} was previously used to indicate the concentration of SCN^{-} ions [32]. Therefore, we calculated the area under the 2126 cm^{-1} band for both healthy and cancer groups to assess which saliva group presented the highest thiocyanate concentration. The results for 30 SERS spectra from each group are presented in Fig. 3b. The analysis indicated that the cancer group displayed an overall higher level of the 2126 cm^{-1} band area. A simple calculus showed that the mean value of the healthy group was 20.03, with a

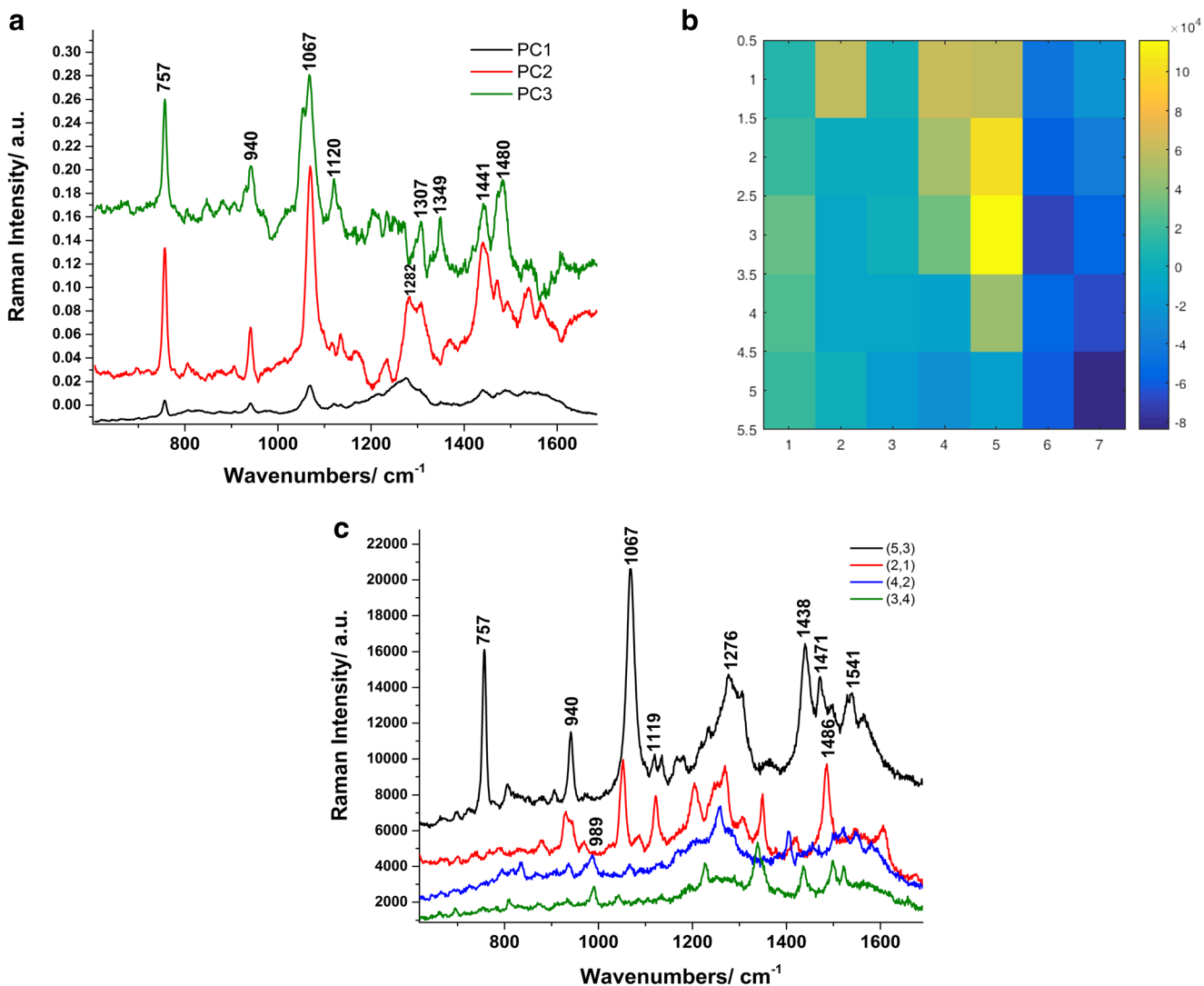**Fig. 2 a** The loadings of the first three principal components characteristic to a healthy volunteer (PC1 90.5%, PC 5%, PC3 2%). PC1 and PC3 were vertically shifted for better visualization. **b** The SERS map reproduced by plotting the score of PC1. The highest intensity is colored in yellow and the lowest intensity in dark blue. **c** SERS spectra collected from random points on the map as indicated in the legend with (x,y) coordinates
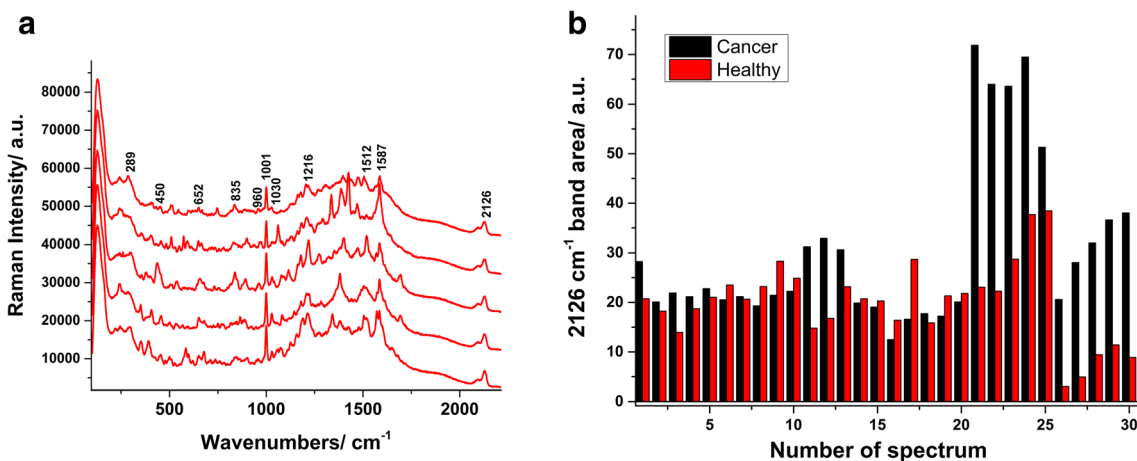

Fig. 3 a Time series SERS spectra acquired at 10s intervals from each other. Excitation 785 nm. **b** Calculated values of the 2126 cm^{-1} band area assigned to thiocyanate, for both healthy and cancer groups

standard deviation of 8.07, while the mean value for the cancer group was 30.41, with a standard deviation of 16.7. It is important to mention that several SERS spectra collected from healthy saliva presented high levels of this band, as well. These spectra (for e.g. the ones numbered 16–25 in Fig. 3b) were collected from smoking volunteers and only part of them showed high values for the 2126 cm^{-1} band area. On the other hand, similar values were obtained from healthy non-smoking volunteers as well (values numbered 11–20 characteristic to non-smoking individuals). Moreover, only some cancerous SERS spectra presented a much higher level of the 2126 cm^{-1} band area (spectra numbered 21–25 in Fig. 3b) compared with the healthy ones, which influences the mean value obtained for the cancer group. Therefore, further studies need to be performed to assess the concentration of this biomarker in the saliva samples and a higher number of volunteers need to be employed for a proper evaluation.

Saliva diagnosis and differentiation

Another aim of this study was to differentiate the saliva collected from healthy individuals from the saliva corresponding to oral cancer patients based on its spectral characteristics. Mean SERS spectra characteristic to each group were calculated based on the extended SERS spectra acquired from both groups and are displayed in Fig. 4a. The shaded region represents the standard deviations from the mean spectra. The thickness of this area suggested the low reproducibility of the SERS spectra, previously observed in the acquired SERS maps, as well. This result indicated that based on the spectral differences between the healthy and oral cancer saliva, diagnosis using SERS is possible. The difference spectrum obtained by subtracting the mean SERS spectrum of the healthy saliva from the one of cancer group further confirmed the

discrepancy of saliva composition between oral cancer and healthy samples (see Fig. 4b). The differences in the SERS data between the oral cancer and healthy groups are given by several main bands located at 2126, 1659, 1585, 1510, 1469, 1390, 1274, 1189, 1093, 820, 631, 483, and 284 cm^{-1}. Qiu et al. previously identified several of these SERS peaks while studying the non-invasive detection of nasopharyngeal cancer and assigned them based on the literature in the field to glycogen at 496 cm^{-1}, tyrosine and lactose at 635 cm^{-1}, phenylalanine at 1003 cm^{-1}, unsaturated fatty acids at 1270 cm^{-1}, collagen and phospholipids at 1448 cm^{-1}, and nucleic acids at 1662 cm^{-1} [20]. Li et al. identified among other bands the 620 cm^{-1} and assigned it to proteins or adenine, the 820 cm^{-1} and the 1280 cm^{-1} peak and assigned them to phospholipids, amide III, proteins, and/or lipids, and the 1390 cm^{-1} band [22]. Furthermore, the appearance of 2126 cm^{-1} band of thiocyanate in the difference spectrum indicated that thiocyanate might play a role as a biomarker in differentiation between healthy and cancerous saliva.

With the aim of differentiating and diagnosing saliva samples in mind, we grouped the two SERS maps presented in Figs. 1 and 2 into one data set and applied PCA to obtain new variables and principal component scores that best explain the differences in the spectra. PCA can classify or organize Raman and SERS data which cannot be visually examined and has contributed significantly to cancer detection, proving to be an invaluable tool for comparing complex biological samples [36].

To illustrate the use of PC scores for diagnosis classification, a comparison between the normal and cancer groups is presented in Fig. 5, as a 3D scatter plot of PC1, PC6, and PC7 on the three axes. For this analysis, the entire spectral range of 600–1720 cm^{-1} was involved from 35 normal saliva SERS spectra and 54 oral cancer saliva SERS spectra. The PCA
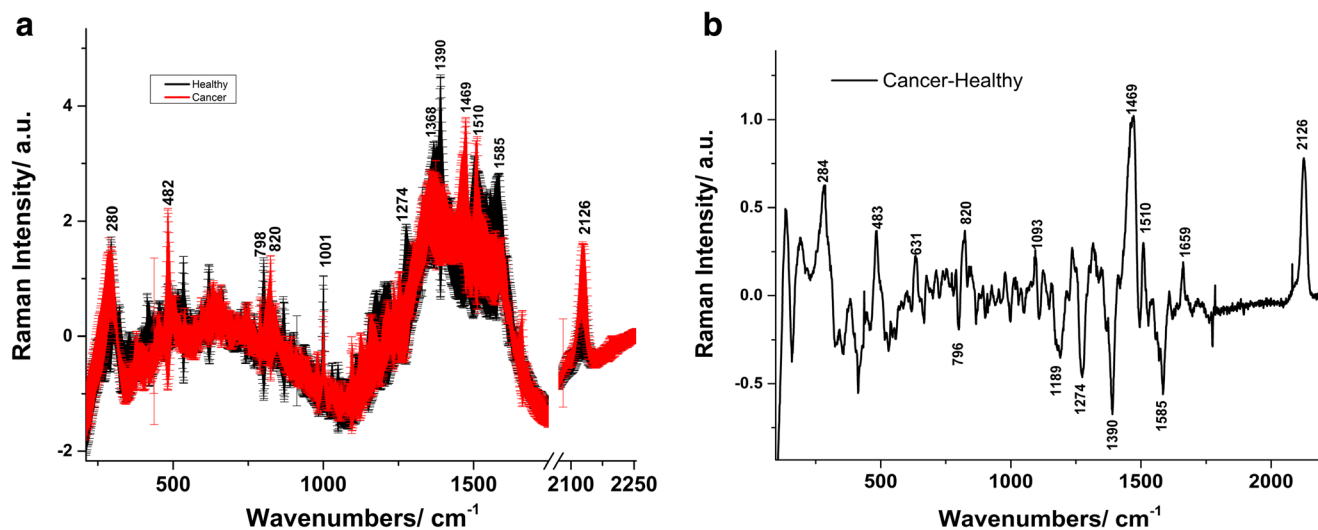

Fig. 4 **a** Mean SERS spectra characteristic to the oral cancer and healthy saliva, respectively. The shaded areas represent the standard deviations of the means. **b** The difference spectrum obtained by subtracting the mean healthy from the mean oral cancer saliva group
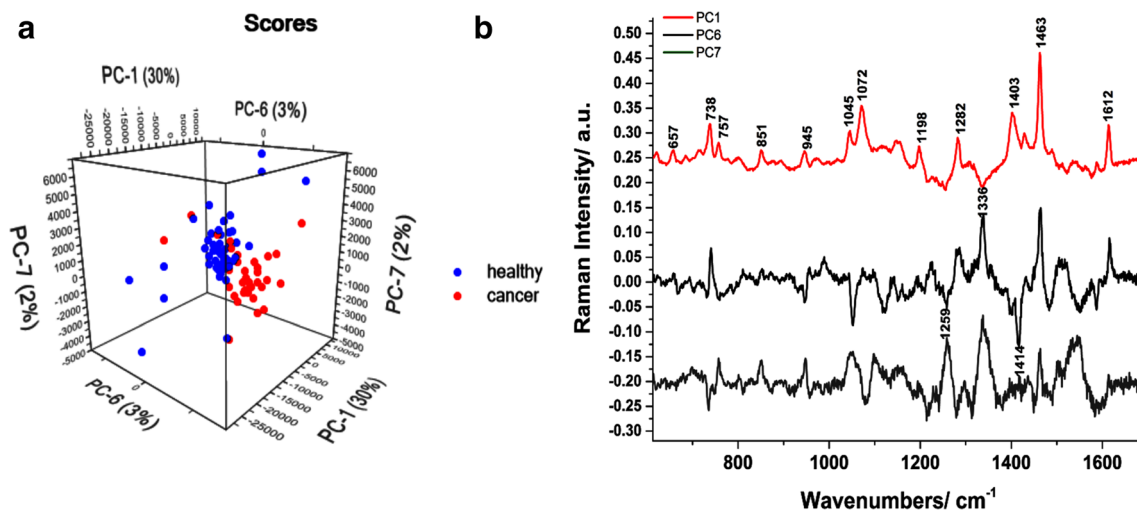
Fig. 5 **a** A three-dimensional scatter plot of the PCA result (scores of PC1 vs PC6 vs PC7) for the oral cancer (red dots) and healthy (blue dots) saliva groups. **b** The loadings of the principal components used for the scatter plot, indicating the SERS bands that contribute most to the separation of the oral cancer saliva from the healthy saliva group

loadings are included in Fig. 5, as well. The PC features corresponded to SERS spectra, showing peaks and troughs at similar positions to those of the spectra. The total variance summed up by the first seven PCs was 82%. PC6 and 7 were used in the 3D scatter plot, together with PC1, as these PCs showed the best separation between the SERS spectra acquired from the two groups. In some cases, a clear distinction between groups is not observed using only the first PCs, as it is possible that these contain no discriminating ability. This does not necessarily mean that there is no distinction between the groups, however, but only that the largest source of variation is similar in both groups. Therefore, looking at higher PCs may result in the expected discrimination. Figure 5a shows that the scores of PC1, PC6, and PC7 for the normal and oral cancer groups, respectively, were distributed in separate axes, forming separate clusters. This demonstrates that we were able to differentiate between the SERS spectra of oral cancer and healthy saliva. The separation of the spectra was due mainly to the 1463 cm^{-1} band assigned to CH_2 bending mode of lipids and proteins, or to sucrose. The other SERS marker bands that contributed to the discrimination of the spectra are indicated in Fig. 5b and are located at 1612, 1414, 1403, 1336, 1259, 1072, and 738 cm^{-1}. These bands are assigned to lipids, fatty acids, nucleic acids, and amino acids such as tyrosine, tryptophan, and proteins, as well as thiocyanate (738 cm^{-1}) [27].

Conclusions

A rapid and easy method for acquiring SERS signal from saliva samples was presented. The method implied simply mixing the saliva supernatant obtained following centrifugation of the sample with Au nanoparticles. The mixture was then dropped onto a clean glass slide and allowed to dry. SERS maps were acquired from both healthy and oral cancer samples. The SERS spectra presented variability of the signal, with fluctuations of the intensity and frequency shifts. However, several reproducible SERS spectra showing well-resolved bands were obtained from regions grouped around an area of the map. We concluded that at these locations the Au nanoparticles cluster together forming hot spots which lead to strong enhancements of the Raman scattering from the biomolecules contained in saliva. The observed SERS bands were mainly assigned to proteins and amino acids. Additionally, thiocyanate, which is known to be a biomarker for human health and smoking status of individuals found in saliva, was distinguished in the SERS spectra and presented an overall higher concentration in the oral cancer samples. The differentiation of the oral cancer saliva samples from the healthy ones was based on PCA, which was able to discriminate between the SERS spectra acquired from the two groups. These investigations prove that the SERS technique can be successfully implemented for the non-invasive, label-free oral cancer detection.

Compliance with ethical standards

Conflict of interest The authors declare that they have no conflict of interest.

Ethical approval All procedures performed in this study were in accordance with the ethical standards of "Iuliu-Hateganu" University of Medicine and Pharmacy in Cluj-Napoca, Romania and with the 1964 Helsinki declaration and its later amendments.

Informed consent Informed consent was obtained from all patients included in the study.

References

1. Warnakulasuriya S (2009) Global epidemiology of oral and oropharyngeal cancer. Oral Oncol 45:309–316. https://doi.org/10.1016/j.oraloncology.2008.06.002
2. Kah JCY, Kho KW, Lee CGL, Richard CJ (2007) Early diagnosis of oral cancer based on the surface plasmon resonance of gold nanoparticles. Int J Nanomedicine 2:785–798
3. Kong K, Kendall C, Stone N, Notingher I (2015) Raman spectroscopy for medical diagnostics — from in-vitro biofluid assays to in-vivo cancer detection. Adv Drug Deliv Rev 89:121–134. https://doi.org/10.1016/j.addr.2015.03.009
4. (2005) Frontmatter. In: Raman spectroscopy for chemical analysis. John Wiley & Sons, Inc, Hoboken, pp i–xxiv
5. Feng S, Chen R, Lin J et al (2010) Nasopharyngeal cancer detection based on blood plasma surface-enhanced Raman spectroscopy and multivariate analysis. Biosens Bioelectron 25:2414–2419. https://doi.org/10.1016/j.bios.2010.03.033
6. Tu Q, Chang C (2012) Diagnostic applications of Raman spectroscopy. Nanomedicine 8:545–558. https://doi.org/10.1016/j.nano.2011.09.013
7. Moskovits M (2005) Surface-enhanced Raman spectroscopy: a brief retrospective. J Raman Spectrosc 36:485–496. https://doi.org/10.1002/jrs.1362
8. Schlücker S (2009) SERS microscopy: nanoparticle probes and biomedical applications. ChemPhysChem 10:1344–1354. https://doi.org/10.1002/cphc.200900119
9. Kneipp J, Kneipp H, McLaughlin M et al (2006) In vivo molecular probing of cellular compartments with gold nanoparticles and nanoaggregates. Nano Lett 6:2225–2231. https://doi.org/10.1021/nl061517x
10. Cinta Pinzaru S, Falamas A, Dehelean CA (2013) Molecular conformation changes along the malignancy revealed by optical nanosensors. J Cell Mol Med 17:277–286. https://doi.org/10.1111/jcmm.12006
11. Simon I, Hedesiu M, Virag P et al (2019) Raman microspectroscopy of dental pulp stem cells: an approach to monitor the effects of cone beam computed tomography low-dose ionizing radiation. Anal Lett 52:1097–1111. https://doi.org/10.1080/00032719.2018.1516771
12. Cialla-May D, Zheng X-S, Weber K, Popp J (2017) Recent progress in surface-enhanced Raman spectroscopy for biological and biomedical applications: from cells to clinics. Chem Soc Rev 46:3945–3961. https://doi.org/10.1039/C7CS00172J
13. Falamas A, Dehelean CA, Cinta Pinzaru S (2018) Monitoring of betulin nanoemulsion treatment and molecular changes in mouse skin cancer using surface enhanced Raman spectroscopy. Vib Spectrosc 95:44–50. https://doi.org/10.1016/j.vibspec.2018.01.004
14. Yoshizawa JM, Schafer CA, Schafer JJ et al (2013) Salivary biomarkers: toward future clinical and diagnostic utilities. Clin Microbiol Rev 26:781–791. https://doi.org/10.1128/CMR.00021-13
15. Bano S, David MP, Indira A (2015) Salivary biomarkers for oral squamous cell carcinoma: an overview. IJSS Case Rep Rev 1:39–45
16. Hu S, Arellano M, Boontheung P et al (2008) Salivary proteomics for oral cancer biomarker discovery. Clin Cancer Res 14:6246–6252. https://doi.org/10.1158/1078-0432.CCR-07-5037
17. Wang S, Qin Y, Zou Z (2016) Determination of liver cancer biomarkers by surface-enhanced Raman scattering using gold-silica nanoparticles. Anal Lett 49:1209–1220. https://doi.org/10.1080/00032719.2015.1098656
18. Cheng Y-S, Rees T, Wright J (2014) A review of research on salivary biomarkers for oral cancer detection. Clin Translat Med 3:3. https://doi.org/10.1186/2001-1326-3-3
19. Zhang C-Z, Cheng X-Q, Li J-Y et al (2016) Saliva in the diagnosis of diseases. Int J Oral Sci 8:133–137. https://doi.org/10.1038/ijos.2016.38
20. Qiu S, Xu Y, Huang L et al (2016) Non-invasive detection of nasopharyngeal carcinoma using saliva surface-enhanced Raman spectroscopy. Oncol Lett 11:884–890. https://doi.org/10.3892/ol.2015.3969
21. Connolly JM, Davies K, Kazakeviciute A et al (2016) Non-invasive and label-free detection of oral squamous cell carcinoma using saliva surface-enhanced Raman spectroscopy and multivariate analysis. Nanomedicine 12:1593–1601. https://doi.org/10.1016/j.nano.2016.02.021
22. Li X (2012) Spectral analysis of human saliva for detection of lung cancer using surface-enhanced Raman spectroscopy. J Biomed Opt 17:037003. https://doi.org/10.1117/1.JBO.17.3.037003
23. Stefancu A, Badarinza M, Moisoiu V et al (2019) SERS-based liquid biopsy of saliva and serum from patients with Sjögren's syndrome. Anal Bioanal Chem. https://doi.org/10.1007/s00216-019-01969-x
24. Feng S, Huang S, Lin D et al (2015) Surface-enhanced Raman spectroscopy of saliva proteins for the noninvasive differentiation of benign and malignant breast tumors. Int J Nanomedicine 10:537–547. https://doi.org/10.2147/IJN.S71811
25. Feng S, Lin D, Lin J et al (2014) Saliva analysis combining membrane protein purification with surface-enhanced Raman spectroscopy for nasopharyngeal cancer detection. Appl Phys Lett 104:073702. https://doi.org/10.1063/1.4866027
26. Hernández-Arteaga A, de Jesús Zermeño Nava J, Kolosovas-Machuca ES et al (2017) Diagnosis of breast cancer by analysis of sialic acid concentrations in human saliva by surface-enhanced Raman spectroscopy of silver nanoparticles. Nano Res 10:3662–3670. https://doi.org/10.1007/s12274-017-1576-5
27. Movasaghi Z, Rehman S, Rehman IU (2007) Raman spectroscopy of biological tissues. Appl Spectrosc Rev 42:493–541. https://doi.org/10.1080/05704920701551530
28. Vargas-Obieta E, Martínez-Espinosa JC, Martínez-Zerega BE et al (2016) Breast cancer detection based on serum sample surface enhanced Raman spectroscopy. Lasers Med Sci 31:1317–1324. https://doi.org/10.1007/s10103-016-1976-x
29. Danciu C, Falamas A, Dehelean C et al (2013) A characterization of four B16 murine melanoma cell sublines molecular fingerprint and proliferation behavior. Cancer Cell Int 13:75. https://doi.org/10.1186/1475-2867-13-75
30. Tsuge K, Kataoka M, Seto Y (2000) Cyanide and thiocyanate levels in blood and saliva of healthy adult volunteers. J Health Sci 46:343–350. https://doi.org/10.1248/jhs.46.343
31. Yang Q, Liang F, Wang D et al (2014) Simultaneous determination of thiocyanate ion and melamine in milk and milk powder using surface-enhanced Raman spectroscopy. Anal Methods 6:8388–8395. https://doi.org/10.1039/C4AY00965G
32. Wu L, Wang Z, Zong S, Cui Y (2014) Rapid and reproducible analysis of thiocyanate in real human serum and saliva using a

droplet SERS-microfluidic chip. Biosens Bioelectron 62:13–18. https://doi.org/10.1016/j.bios.2014.06.026

33. Wang P, Li H, Cui C, Jiang J (2019) In situ surface-enhanced Raman spectroscopy study of thiocyanate ions adsorbed on silver nanoparticles under high pressure. Chem Phys 516:1–5. https://doi.org/10.1016/j.chemphys.2018.08.029

34. Feng Y, Mo R, Wang L et al (2019) Surface enhanced Raman spectroscopy detection of sodium thiocyanate in milk based on the aggregation of Ag nanoparticles. Sensors 19:1363. https://doi.org/10.3390/s19061363

35. Shiue I (2015) Urinary thiocyanate concentrations are associated with adult cancer and lung problems: US NHANES, 2009–2012.

Environ Sci Pollut Res 22:5952–5960. https://doi.org/10.1007/s11356-014-3777-8

36. Bonnier F, Byrne HJ (2012) Understanding the molecular information contained in principal component analysis of vibrational spectra of biological systems. Analyst 137:322–332. https://doi.org/10.1039/C1AN15821J

Publisher's note Springer Nature remains neutral with regard to jurisdictional claims in published maps and institutional affiliations.